Nationwide increase of polycyclic aromatic hydrocarbons in ultrafine particles during winter over China

Qingqing Yu[a], Xiang Ding[a,d,*], Quanfu He[a], Weiqiang Yang[e], Ming Zhu[a,b], Sheng Li[a,b], Runqi Zhang[a,b], Ruqin Shen[a], Yanli Zhang[a,c,d], Xinhui Bi [a,d], Yuesi Wang[c,f], Ping'an Peng[a,d], Xinming Wang[a,b,c,d,*]

[a]State Key Laboratory of Organic Geochemistry and Guangdong Key Laboratory of Environmental Protection and Resources Utilization, Guangzhou Institute of Geochemistry, Chinese Academy of Sciences, Guangzhou 510640, China

[b]University of Chinese Academy of Sciences, Beijing 100049, China

[c]Center for Excellence in Regional Atmospheric Environment, Institute of Urban Environment, Chinese Academy of Sciences, Xiamen 361021, China

[d]Guangdong-Hong Kong-Macao Joint Laboratory for Environmental Pollution and Control, Guangzhou Institute of Geochemistry, Chinese Academy of Science, Guangzhou 510640, China

[e]Guangdong Provincial Academy of Environmental Science, Guangzhou 510045, China

[f]State Key Laboratory of Atmospheric Boundary Layer Physics and Atmospheric Chemistry, Institute of Atmospheric Physics, Chinese Academy of Sciences, Beijing 100029, China

*corresponding author:

Dr. Xinming Wang and Dr. Xiang Ding

State Key Laboratory of Organic Geochemistry Guangzhou Institute of Geochemistry, Chinese Academy of Sciences, 511 Kehua Rd, Tianhe, Guangzhou, 510640, China.

Email addresses: wangxm@gig.ac.cn and xiangd@gig.ac.cn

Abstract

Polycyclic aromatic hydrocarbons (PAHs) are toxic compounds in the atmosphere and have adverse effects on public health, especially through the inhalation of particulate matter (PM). At present, there are limited understandings in size distribution of particulate-bound PAHs and its health risk on a continental scale. In this study, we carried out simultaneously PM campaign from October, 2012 to September, 2013 at 12 sampling sites including urban, sub-urban and remote sites in different regions of China. Size-segregated PAHs and typical tracer of coal combustion (picene), biomass burning tracer (levoglucosan) and vehicle exhaust (hopanes) were measured. The annual averages of total 24 PAHs ($\sum_{24}$PAHs) and benzo[a]pyrene (BaP) carcinogenic equivalent concentration (BaP_{eq}) ranged from 7.56 to 205 ng m^{-3} with a mean of 53.5 ng m^{-3} and 0.21 to 22.2 ng m^{-3} with a mean of 5.02 ng m^{-3}, respectively. At all the sites, $\sum_{24}$PAHs and BaP_{eq} were dominated in the ultrafine particles with aerodynamic diameter <1.1 μm, followed by those in the size ranges of 1.1-3.3 μm and >3.3 μm. Compared with the southern China, the northern China witnessed much higher $\sum_{24}$PAHs (87.36 ng m^{-3} vs. 17.56 ng m^{-3}), BaP_{eq} (8.48 ng m^{-3} vs. 1.34 ng m^{-3}) and PAHs inhalation cancer risk (7.4×10^{-4} vs. 1.2×10^{-4}). Nationwide increases in both PAH levels and inhalation cancer risk occurred in winter. The unfavorable meteorological conditions and enhanced emissions of coal combustion and biomass burning together led to severe PAHs pollution and high cancer risk in the atmosphere of the northern China, especially during winter. Coal combustion is the major source of BaP_{eq} in all size particles at most sampling sites. Our results suggested that the reduction of coal and biofuel consumption in the residential sector could be crucial and effective to lower PAH concentrations and its inhalation cancer risk in China.

45 **Key words**: Polycyclic aromatic hydrocarbons; China; inhalation cancer risk; coal combustion;

46 biomass burning

47

1. Introduction

Ambient particulate matter (PM) pollution has adverse effects on public health. The global deaths caused by exposure to the PM with aerodynamic diameters less than 2.5 μm ($PM_{2.5}$) kept increasing from 1990 and reached 4.2 million in 2015 (Cohen et al., 2017). In China, ambient $PM_{2.5}$ pollution ranked the fourth leading risks for deaths (Yang et al., 2013), and caused 1.7 million premature deaths in 2015 (Song et al., 2017). Adverse health impacts of PM are associated with particle size and chemical components (Chung et al., 2015; Dong et al., 2018). Higher risk of cardiovascular disease was associated with smaller size-fractioned particulate matter, especially $PM_{1.0}$-bound particulate matter (Yin et al., 2020).

Polycyclic aromatic hydrocarbons (PAHs) are a group of organic substances composed of two or more aromatic rings. Due to the mutagenic, teratogenic, and carcinogenic properties (Kim et al., 2013), PAHs are one of the most toxic components in PM (Xu et al., 2008). Toxic PAHs usually enrich in fine particles, especially the aerodynamic diameters less than 1.0 μm (Wang et al., 2016; Li et al., 2019) which can enter the human respiratory system through inhalation (Yu et al., 2015). Exposure to PAHs likely induces DNA damage and raises the risk of gene mutation (Zhang et al., 2012; Lv et al., 2016) and cardiopulmonary mortality (Kuo et al., 2003; John et al., 2009). Previous studies have demonstrated that inhalation exposure to PAHs can cause high risk of lung cancer (Armstrong et al., 2004; Zhang et al., 2009; Shrivastava et al., 2017).

Atmospheric PAHs are mainly emitted from incomplete combustion of fossil fuels and biomasses (Mastral and Callen, 2000). As typical semi-volatile chemicals, PAHs can transport over long distances (Zelenyuk et al., 2012) and have been detected in the global atmosphere (Brown et al., 2013; Garrido et al., 2014; Hong et al., 2016; Liu et al., 2017a; Hayakawa et al.,

2018). Emission inventory indicated that developing countries were the major contributors to global PAHs emission (Zhang and Tao, 2009; Shen et al., 2013a).

As the largest developing country in the world, China has large amounts of PAHs emission and high cancer risk caused by PAHs exposure. The annual emission of 16 USEPA priority PAHs in China sharply increased from 18 Gg in 1980 to 106 Gg in 2007 (Xu et al., 2006; Shen et al., 2013a). China became the largest emitter of PAHs, accounting for about 20% of the global PAHs emission during 2007 (Shen et al., 2013a). The excess lung cancer risk caused by inhalation exposure to ambient PAHs was estimated to be 6.5×10^{-6} in China (Zhang et al., 2009), which was 5.5 times higher than the acceptable risk level of 1.0×10^{-6} in US (USEPA, 1991). As Hong et al. (2016) estimated, the lifetime excess lung cancer cases caused by exposure to PAHs for China ranged from 27.8-2200 per million people and were higher than other Asia counties.

Moreover, PAHs emission and cancer risk in China have large spatial and seasonal variations. As reported by Tao and coworkers, high emission of PAHs occurred in the North China Plain (Zhang et al., 2007), and the emission in winter was 1.6 times higher than that in summer (Zhang and Tao, 2008). Thus, the lung cancer risk caused by ambient PAH inhalation exposure in the northern China was higher than that in the southern China (Zhang et al. 2009). In addition, through long-range atmospheric transport, PAHs emitted in China could spread to other regions of the world (Zhang et al., 2011; Inomata et al., 2012).

For more accurate estimation of inhalation exposure to ambient PAHs and its cancer risks in China, it is essential to carry out nationwide campaigns to acquire spatial and seasonal characteristics of atmospheric PAHs. The data of PAHs in the ambient air are accumulating in China during the past decades. Among these filed studies, most were conducted in rapidly

93 developing economic regions, including the North China region (Huang et al., 2006; Liu et al.,
94 2007a; Wang et al., 2011; Lin et al., 2015a; Lin et al., 2015b; Tang et al., 2017; Yu et al., 2018),
95 Yangtze River Delta region (Liu et al., 2001; Zhu et al., 2009; Gu et al., 2010; He et al., 2014)
96 and Pearl River Delta region (Bi et al., 2003; Guo et al., 2003; Li et al., 2006; Tan et al., 2006;
97 Duan et al., 2007; Lang et al., 2007; Yang et al., 2010; Gao et al., 2011, 2012, 2013, 2015; Yu
98 et al., 2016), due to large amounts of combustion emission and high density of population in
99 these regions. These studies provided insight into the fate and health risk of airborne PAHs on
100 a local or regional scale. However, due to the inconsistency in sampling methods, frequency
101 and duration in these local and regional campaigns, it is difficult to draw a national picture of
102 PAHs pollution in the air of China.

103 There are rare dataset discovering nationwide characteristics of airborne PAHs over China.
104 Liu et al. (2007b) reported PAHs in the air of 37 cities across China using passive polyurethane
105 foam (PUF) disks. Wang et al. (2006) and Liu et al., (2017b) determined $PM_{2.5}$-bound PAHs
106 over 14 and 9 Chinese cities, respectively. PAHs in the total suspended particle (TSP) and gas
107 phase were measured over 11 cities in China (Ma et al., 2018; Ma et al., 2020). Besides these
108 important information of PAHs in the bulk PM, it is vital to determine size distribution of PAHs,
109 since the size of particles is directly linked to their potential for causing health problems. On
110 the national scale, at present, there is only one field study available reporting size-segregated
111 atmospheric PAHs at 10 sites (Shen et al., 2019). Therefore, it is essential to carry out large
112 range campaigns coving multiple types of sites across different regions to investigate size
113 distribution of PAHs levels and sources and discover their difference in health risks among
114 typical regions of China (e.g. north vs. south, urban vs. remote). In this study, we

simultaneously collected filter-based size-fractionated PM samples consecutively at 12 sites for one year. We analyzed chemical compositions of PAHs as well as other organic tracers to characterize the spatiotemporal pattern and size distribution of PAHs over China and to explore the possible sources of PAHs on the national scale. This information is helpful to provide a basis for PAHs pollution control and health effects reduction in different regions of China.

2. Materials and Methods

2.1 Field sampling

The PM samples were collected simultaneously at 12 sampling sites across 6 regions of China, containing five urban sites, three sub-urban sites and four remote sites (Figure S1 and Table S1 in the supporting information). The Huai River-Qin Mountains Line is the geographical line that divides China into the northern and southern regions. There are central heating systems in winter in some urban areas of the northern China, but not so in the southern China. The 12 sampling sites are Beijing (BJ), Dunhuang (DH), Hefei (HF), Hailun (HL), Kunming (KM), Qianyanzhou (QYZ), Sanya (SY), Shapotou (SPT), Taiyuan (TY), Tongyu (TYU), Wuxi (WX) and Xishuangbanna (BN). According to their locations, 6 of the 12 sites are situated in the northern China, including BJ, DH, HL, SPT, TY and TYU. And the remaining 6 sites are located in the southern China, including BN, HF, KM, QYZ, SY and WX.

Total suspended particles (TSP) were collected using Anderson 9-stage cascade impactors (<0.4, 0.4-0.7, 0.7-1.1, 1.1-2.1, 2.1-3.3, 3.3-4.7, 4.7-5.8, 5.8-9.0, >9.0 μm) at a constant flow of 28.3 L/min. Quartz fiber filters (Whatman, QMA) that were used to collect PM samples were prebaked for 8 h at 450 ℃. At each site, one set of nine size-fractionated PM samples were collected for 48-hr every 2 weeks. 294 sets of field samples and one set of field blanks were

137 collected. Detailed information of the field sampling can be found elsewhere (Ding et al., 2014).
138 According to the meteorological definition, each season lasts three months that spring runs from
139 March to May, summer runs from June to August, fall (autumn) runs from September to
140 November, and winter runs from December to February.

141 The data of average temperature (T), relative humidity (RH), the maximum solar radiation
142 (SR) during each sampling episode were available in the China Meteorological Data Service
143 Center (http://data.cma.cn/en). And the average boundary layer height (BLH) was calculated
144 using the NOAA's READY Archived Meteorology online calculating program
145 (http://ready.arl.noaa.gov/READYamet.php).

146 2.2 Chemical analysis

147 Each set of nine filters were combined into three samples with the aerodynamic diameters
148 smaller than 1.1 μm ($PM_{1.1}$), between 1.1 μm and 3.3 μm ($PM_{1.1\text{-}3.3}$), and large than 3.3 μm
149 ($PM_{>3.3}$), respectively. Before ultrasonic solvent extraction, 400 ul of isotope-labeled mixture
150 compounds (tetracosane-d_{50}, napthalene-d_8, acenaphthene-d_{10}, phenethrene-d_{10}, chrysene-d_{12},
151 perylene-d_{12} and levoglucosan-$^{13}C_6$) were spiked into the samples as internal standards.
152 Samples were ultrasonic extracted twice with the mixed solvent of dichloride methane / hexane
153 (1:1, v/v), and then twice with the mixed solvent of dichloride methane / methanol (1:1, v/v).
154 The extracts of each sample were filtered, combined, and finally concentrated to about 1 mL.
155 Then the extracts were divided into two aliquots for silylation and methylation, respectively.
156 Detailed information about the procedures of silylation and methylation were introduced
157 elsewhere (Ding et al., 2014; Yu et al., 2016).

158 The methylated aliquot was analyzed for PAHs and hopanes using a 7890/5975C gas

chromatography/mass spectrometer detector (GC/MSD) in the selected ion monitoring (SIM) mode with a 60 m HP-5MS capillary column (0.25 mm, 0.25 μm). The GC temperature was initiated at 65 ℃, held for 2 min, and then increased to 300 ℃ at 5 ℃ min^{-1} and held for 40 min. The silylated aliquot was analyzed for levoglucosan using the same GC/MSD in the scan mode with a 30 m HP-5MS capillary column (0.25 mm, 0.25 μm). The GC temperature was initiated at 65 ℃, held for 2 min, and then increased to 290 ℃ at 5 ℃ min^{-1} and held for 20 min. The target compounds were identified by authentic standards and quantified using an internal calibration approach. Table S2 lists the 24 target PAHs and their abbreviations.

2.3 Quality control and quality assurance

Field and laboratory blanks were analyzed in the same manner as the PM samples. The target compounds were not detected or negligible in the blanks. The data reported in this study were corrected by corresponding field blanks. To test the recovery of the analytical procedure, we analyzed the NIST urban dust Standard Reference Material (SRM 1649b, n=6) in the same manner as the PM samples. Compared with the certified values for PAHs in SRM 1649b, the recoveries were 81.5±1.9%, 66.6±5.4%, 113.6±4.4%, 76.2±2.5%, 100.4±7.9%, 138.3±3.6%, 109.5±14.2%, 125.8±8.8% and 86.4±10.7% for Pyr, Ret, Chr, BbF, BkF, BeP, Per, IcdP and Pic respectively. The data reported in this study were not recovery corrected. The method detection limits (MDLs) of the target compounds ranged from 0.01 to 0.08 ng m^{-3}.

2.4 Positive matrix factorization (PMF) analysis

Positive matrix factorization (PMF) (USEPA, version PMF 5.0) was employed for source apportionment of PAHs. The model has been widely used to attribute major sources of PAHs (Larsen and Baker, 2003; Belis et al., 2011). In case the observed concentration (*Con*) of a

compound was below its MDL, half of the MDL was used as the model input data and the uncertainty (*Unc*) was set as 5/6 of the MDL (Polissar et al., 1998). If the *Con* of a compound was higher than its MDL, *Unc* was calculated as $Unc = [(20\% \times Con)^2 + (MDL)^2]^{1/2}$ (Polissar et al., 1998).

2.5 Exposure assessment

Besides BaP, other PAHs like BaA, BbF, DahA and IcdP are also carcinogenic compounds (IARC, 2001). In order to assess the carcinogenicity of bulk PAHs, the BaP carcinogenic equivalent concentration (BaP_{eq}) was calculated by multiplying the concentrations of PAH individuals (PAH_i) with their toxic equivalency factor (TEF_i) as:

$$BaP_{eq} = \sum_{i=1}^{n} PAH_i \times TEF_i \quad (1)$$

In this study, we adopted the TEFs reported by Nisbet and Lagoy (1992) which were 0.001 for Phe, Flu and Pyr, 0.01 for Ant, Chr and BghiP, 0.1 for BaA, BbF, BkF, BeP, and IcdP, and 1.0 for BaP and DahA. Table S3 lists annual averages of PAH individuals and BaP_{eq} at the 12 sites.

Incremental lifetime lung cancer risk (ILCR) caused by inhalation exposure to PAHs was estimated as:

$$ILCR = BaP_{eq} \times UR_{BaP} \quad (2)$$

where UR_{BaP} is the unit relative risk of BaP. Based on the epidemiological data from studies in coke-oven workers, the lung cancer risk of BaP inhalation was estimated to be 8.7×10^{-5} per ng m^{-3} (WHO, 2000). Thus, we used a UR_{BaP} value of 8.7×10^{-5} per ng/m^3 in this study.

3. Results and discussion

3.1 General marks

Annual averages of the total 24 PAHs ($\sum_{24}$PAHs) in TSP (sum of three PM size ranges) ranged from 7.56 to 205 ng m^{-3} (Figure 1a) among the 12 sampling sites with a mean of 53.5 ng m^{-3}. The highest concentration of $\sum_{24}$PAHs was observed at TY and the lowest level occurred at SY (Figure 1a). Compared with the data in other large scale observations (Table 1), atmospheric concentrations of PAHs measured at the 12 sites in this study were comparable with previously reported values in China in 2013-2014 (Liu et al., 2017b; Shen et al., 2019) and U.S. (Liu et al., 2017a), lower than those measured in China in 2003 and 2008-2009 (Wang et al., 2006; Ma et al., 2018), but higher than those over Great Lakes (Sun et al., 2006), Europe (Jaward et al., 2004), Japan (Hayakawa et al., 2018) and some Asian countries (Hong et al., 2016). Figure 1a also presents the compositions of PAHs. Apparently, 4- and 5-rings PAHs were the majority in $\sum_{24}$PAHs with the mass shares of 36.8±5.6% and 31.4±9.6%, respectively, followed by the PAHs with 3-rings (19.2±9.4%), 6-rings (11.3±3.8%), and 7-rings (1.3±0.6%). The concentrations of $\sum_{24}$PAHs at urban sites (82.7 ng m^{-3}) were significant higher ($p<0.05$) than those at sub-urban (48.0 ng m^{-3}) and remote sites (18.0 ng m^{-3}) (Figure S2).

Annual averages of BaP in TSP among the 12 sites were in the range of 0.09 to 11.0 ng m^{-3} with a mean of 2.58 ng m^{-3}. The highest level of atmospheric BaP occurred at TY and the lowest existed at SY. The BaP values at five sites (WX, BJ, HL, DH and TY) exceeded the national standard of annual atmospheric BaP (1.0 ng m^{-1}) by factors of 1.2 to 11.0. For BaP_{eq}, annual averages ranged from 0.21 to 22.2 ng m^{-3} with the predominant contribution from 5-rings PAHs (Figure 1b). ILCR caused by inhalation exposure to PAHs ranged from 1.8×10^{-5} (SY) -1.9×10^{-3} (TY) among the 12 sites in China (Figure S3), which were much higher than the acceptable risk level of 1.0×10^{-6} in US (USEPA, 1991). All these demonstrated that China faced

225 severe PAHs pollution and high health risk (Zhang et al., 2009; Shrivastava et al., 2017). And
226 BeP_{eq} (Figure S4) and ILCR (Figure S5) were both the highest at urban sites. All these indicated
227 that people in urban regions of China were faced with higher exposure risk of PAHs pollution
228 as compared to those in rural and remote areas. Figure S6 exhibits that 4- and 5-rings PAHs are
229 the majority in $\sum_{24}$PAHs at urban, sub-urban and remote sites, which totally accounted 72.2%,
230 63.8% and 66.6% of the total amounts in TSP, respectively. The percentage of 5-rings PAHs
231 dominates at urban sites, and 4-rings PAHs makes the largest proportion at sub-urban and
232 remote sites (Figure S6).

233 **3.2 Enrichment of PAHs in $PM_{1.1}$**

234 Figure 2 presents the size distribution of PAHs and BaP_{eq} at the 12 sites in China. Both
235 $\sum_{24}$PAHs and BaP_{eq} were concentrated in $PM_{1.1}$, accounting for 44.6-71.3% and 56.7-79.3% of
236 the total amounts in TSP, respectively. And BaP_{eq} had more enrichment in $PM_{1.1}$ than $\sum_{24}$PAHs.
237 The mass fractions of $\sum_{24}$PAHs and BaP_{eq} in $PM_{1.1\text{-}3.3}$ were 20.6-39.5% and 16.1-38.3%. The
238 coarse particles ($PM_{>3.3}$) had the lowest loadings of $\sum_{24}$PAHs (7.2-23.4%) and BaP_{eq} (3.0-
239 12.9%). Thus, our observations indicated that PAHs in the ultrafine particles ($PM_{1.1}$) contributed
240 most health risk of PAHs in TSP over China. A previous study at three sites in East Asia found
241 that size distribution of PAHs was unimodal and peaked at 0.7-1.1 μm size (Wang et al., 2009).
242 A recent study at 10 sites of China also found that PAHs were concentrated in $PM_{1.1}$ (Shen et
243 al., 2019). Based on the observation at one site in the Fenhe Plain, northern China, Li et al.
244 (2019) pointed out that PAHs in the particles with the aerodynamic diameters <0.95 μm
245 contributed more than 60% to the total cancer risk of PAHs in PM_{10}. All these results
246 demonstrate that high carcinogenicity of PAHs is accompanied with ultrafine particles,

probably because small particles are apt to invade the blood vessels and cause DNA damage. Thus, further studies should put more attentions on PAHs pollution in ultrafine particles.

Figure S7 and Figure S8 show seasonal variations in size distribution of $\sum_{24}$PAHs and BaP_{eq}, respectively. $\sum_{24}$PAHs and BaP_{eq} were enriched in $PM_{1.1}$ throughout the year at all sites. The mass fractions of $\sum_{24}$PAHs and BaP_{eq} in $PM_{1.1}$ were the highest during fall to winter (up to 74.6% and 79.7% at the DH site), and the lowest during summer (down to 39.2% and 50.7% at the BN site). It should be related to the emission sources of PAHs. Atmospheric PAHs are mainly derived from combustion sources. As Shen et al. (2013b) reported, PAHs emitted form biomass burning and coal combustion enriched in ultrafine particles (<1.1 μm). Moreover, coal combustion witnessed more enrichment of PAHs in ultrafine particles than biomass burning. Figure S9 presents monthly variations in size distribution of PAHs with different number of rings. The mass shares of 3-rings PAHs in $PM_{1.1}$ (39.2%), $PM_{1.1\text{-}3.3}$ (32.0%) and $PM_{>3.3}$ (28.9%) were comparable. And the highest loading of 3-rings PAHs in $PM_{1.1}$ was observed in December 2012. The mass fractions of 4-ring PAHs in $PM_{1.1}$ were the highest in December 2012 (58.4%) and the lowest in July 2013 (39.5%). The higher molecular weight PAHs (5-7 rings PAHs) were enriched in $PM_{1.1}$ throughout the year.

3.3 High levels of atmospheric PAHs in the northern China

Figure 3 shows the differences of atmospheric PAHs between the northern China (BJ, DH, HL, SPT, TY and TYU) and southern China (BN, HF, KM, QYZ, SY and WX). $\sum_{24}$PAHs in the northern China was higher than that in the southern China by a factor of 5.0 (Figure 3a). The concentrations of PAHs with different ring number were all higher in the northern China than those in the southern China, especially for the 4-7 rings PAHs. Moreover, BaP、BaP_{eq} and

ILCR in the northern China were 5.8, 5.3 and 5.3 times higher than those in the southern China (Figure 3b). The higher concentrations of PAHs in the air of the northern China than the southern China were also reported in previous field studies (Liu et al., 2017b; Ma et al., 2018; Shen et al., 2019). Based on the emission inventories and model results, previous studies predicted that PAHs concentrations, BaP levels and lung cancer risk of exposure to ambient PAHs in the northern China were all higher than those in the southern China (Xu et al., 2006; Zhang et al., 2007; Zhang and Tao, 2009; Zhu et al., 2015). All these indicated much higher PAHs pollution and health risk in the northern China.

The northern-high feature of atmospheric PAHs should be determined by the meteorological conditions and source emissions. Theoretical relationship between meteorological parameters (temperature, solar radiation and boundary layer height) and the concentration of particulate-bound PAHs were discussed, the detail theoretical discussion information can be found in Text S1 in the supporting information. We illustrate that decrease of ambient temperature would result in the increase of individual PAH in the particulate phase assuming a constant total concentration in the air. The decrease of SR can indeed lower concentrations of hydroxyl radical [OH] and accumulate PAHs in the air, resulting in the increase of PAHs concentrations. And low height of boundary layer can inhibit the vertical diffusion of PAHs, which leads to PAHs accumulation and increased concentrations. As Figure 4 showed, PAHs exhibited strong negative correlations with temperature (T), solar radiation (SR) and the boundary layer height (BLH), especially in the northern China. This indicated that the unfavorable meteorological conditions, such as low levels of temperature, solar radiation and BLH could lead to PAHs accumulation in the air (Sofuoglu et al., 2001; Callén et al., 2014;

291 Lin et al., 2015a; Li et al., 2016a). In fact, annual averages of T, SR and BLH in the northern
292 China were all significant lower than those in the southern China ($p<0.05$, Table S4), which
293 could indeed cause the accumulation of PAHs in the air of the northern China. In addition, low
294 temperature in the northern China would promote the condensation of semi-volatile PAHs on
295 particles (Wang et al., 2011; Ma et al., 2020). At the southern sites, the negative correlations
296 between PAHs and meteorological parameters (SR and BLH) were not as strong as those in the
297 northern sites. This implied that the adverse influence of meteorological conditions on PAHs
298 pollution in the southern China might be less significant than that in the northern China. Then
299 we divide the one-year data into warm and cold seasons based on the ambient temperature. As
300 Figure S10 showed, at most sites in the northern and southern China, PAHs negatively
301 correlated with temperature (T), boundary layer height (BLH) and solar radiation (SR) in both
302 cold ($T < 10$ ° C) and warm ($T > 10$ ° C) seasons. Thus, coupled with theoretical discussion, we
303 suggested that worsened PAH pollution in winter partly caused by adverse meteorological
304 conditions.

305 For PAHs emission, there are apparent differences in sources and strength between the
306 northern and southern regions. For instance, there is central heating during winter in the
307 northern China, but not so in the southern China. The residential heating during cold period in
308 the northern China could consume large amounts of coal and biofuel, and release substantial
309 PAHs into the air (Liu et al., 2008; Xue et al., 2016). Consequently, atmospheric levels of PAHs
310 in the northern China were much higher than those in the southern China. Since central heating
311 systems start heat supply simultaneously within each region in the northern China, atmospheric
312 PAHs should increase synchronously within the northern regions of China. To check the spatial

homogeneity of PAHs on a regional scale, we analyzed the correlation of PAHs between paired sites within each region. As Table 2 exhibited, PAHs varied synchronously and correlated well at the paired sites in the northern China ($p<0.001$). And closer distance between sites, stronger correlations were observed. The spatial synchronized trends of PAHs observed in the northern regions of China probably resulted from the synchronous variation of PAHs emission in the northern China. In the southern China, although the distances between paired sites were closer than those in the northern regions, the correlations between sites within a region was weaker. This indicated that there might be more local emission which sources and strength vary place to place in the southern China.

We applied diagnostic ratios of PAH isomers to identify major sources of atmospheric PAHs. The ratios of IcdP/(IcdP+BghiP) and Flu/(Flu+Pyr) have been widely used to distinguish possible sources of PAHs (Aceves and Grimalt, 1993; Zhang et al., 2005; Ding et al., 2007; Gao et al., 2012; Lin et al., 2015a; Ma et al., 2018). As summarized by Yunker et al. (2002), the petroleum boundary ratios for IcdP/(IcdP+BghiP) and Flu/(Flu+Pyr) are close to 0.20 and 0.40, respectively; for petroleum combustion, the ratios of IcdP/(IcdP+BghiP) and Flu/(Flu+Pyr) range from 0.20 to 0.50 and 0.40 to 0.50, respectively; and the combustions of grass, wood and coal have the ratios higher than 0.50 for both IcdP/(IcdP+BghiP) and Flu/(Flu+Pyr). As Figure 5 showed, the ratios of Flu/(Flu+Pyr) at the 12 sites ranged from 0.49 to 0.76, suggesting that biomass (grass/wood) burning and coal combustion were the major sources. And the ratios of IcdP/(IcdP+BghiP) were in the range of 0.32 to 0.62, indicating that besides biomass and coal combustion, petroleum combustion, especially vehicle exhaust was also an important source of atmospheric PAHs. Thus, as identified by the diagnostic ratios, biomass burning, coal

combustion and petroleum combustion were major sources of atmospheric PAHs over China. This is also confirmed by the significant correlations of $\sum_{24}$ PAHs with the typical tracers of biomass burning (levoglucosan), coal combustion (picene) and vehicle exhaust (hopanes) at most sites (Figure 6). As global emission inventories showed, PAHs in the atmosphere were mainly released from the incomplete combustion processes including coal combustion, biomass burning and vehicle exhaust (Shen et al., 2013a).

To further attribute PAHs sources, we employed the PMF model to quantify source contributions to atmospheric PAHs at the 12 sites in China. Three factors were identified, and the factor profile resolved by PMF were presented in Figure S11. The first factor was identified as biomass burning, as it had high loadings of the biomass burning tracer, levoglucosan and light weight molecular PAHs such as Phe, Ant, Flu and Pyr which are largely emitted from biomass burning (Li et al., 2016b). The second factor was considered to be coal combustion, as it was characterized by high fractions of the coal combustion marker, picene and the high molecular weight PAHs (Shen et al., 2013b). The third factor was regarded as vehicle exhaust, as it was featured by presence of hopanes, which are molecular markers tracking vehicle exhaust (Cass, 1998; Dai et al., 2015). As Figure S12 showed, there was significant agreement between the predicted and measured PAHs at each site (R^2 in the range of 0.78 to 0.99, $p<0.001$). As the emission inventory of PAHs in China showed, residential/commercial, industrial and transportation were the major sectors of atmospheric PAHs in 2013 (Figure S13, http://inventory.pku.edu.cn). Residential/commercial and industrial sectors mainly consumed coal and biofuel while transportation consumed oil (Shen et al., 2013a). Thus, the mainly sources of PAHs in China were coal combustion, biomass burning and petroleum combustion

(especially vehicle exhaust).

Figure 7a presents atmospheric PAHs emitted from different sources in China. In the northern China, coal combustion was the major source of atmospheric PAHs (73.6 ng m^{-3}, 84.2% of $\sum_{24}$PAHs), followed by biomass burning (11.8 ng m^{-3} and 13.5%) and vehicle exhaust (2.0 ng m^{-3} and 2.3%). In the southern China, coal combustion (9.6 ng m^{-3} and 54.8%) and biomass burning (6.8 ng m^{-3} and 39.0%) were the major contributors, followed by vehicle exhaust (1.1 ng m^{-3} and 6.2%). Atmospheric PAHs emitted from the three sources in the northern China were all higher than those in the southern China, especially from coal combustion. Thus, coal combustion was the most important source of atmospheric PAHs in China and caused large increases in PAHs pollution in the northern China. As China statistics yearbook recorded (http://www.stats.gov.cn/english/Statisticaldata/AnnualData/), coal was the dominant fuel in China, accounting for 70.6% (24.1×10^8 tons of Standard Coal Equivalent, SCE) of total primary energy consumption in 2012, followed by crude oil 19.9% (6.7×10^8 tons of SCE) and other types of energy 9.5%, including biofuel, natural gas, hydro power, nuclear power and other power (3.2×10^8 tons of SCE). Although the biofuel consumption was lower than crude oil, the poor combustion conditions during residential biofuel burning could led to higher PAHs emissions as compared to petroleum combustion.

We further compared our results with those in the PAHs emission inventory of China (http://inventory.pku.edu.cn) (Figure S14). Our source apportionment results focused on fuel types, while the emission inventory classified the sources into 6 socioeconomic sectors (residential & commercial activities, industry, energy production, agriculture, deforestation & wildfire, and transportation). Since the transportation mainly used liquid petroleum (gasoline

379 and diesel) and the rest sectors mainly consumed solid fuels (coal and biomass), we grouped
380 these sectors into liquid petroleum combustion and solid fuel burning to directly compare with
381 our results. As Figure S14 showed, both our observation and emissions inventory demonstrated
382 that the PAHs contributions from solid fuel burning was higher in the northern China, while the
383 PAHs contributions from liquid petroleum combustion was higher in the southern China.

384 Atmospheric PAHs emitted from different sources at urban, sub-urban and remote sites
385 (Figure 7b) and different size particles (Figure 7c) were discussed. At urban and sub-urban sites,
386 coal combustion was the largest source of $\sum_{24}$PAHs (70.4 ng m^{-3}, 85.1% and 30.5 ng m^{-3}, 63.5%),
387 followed by biomass burning (10.1 ng m^{-3}, 12.2% and 16.3 ng m^{-3}, 33.9%) and vehicle emission
388 (2.2 ng m^{-3}, 2.6% and 1.2 ng m^{-3}, 2.5%), while at remote sites the contributions of coal
389 combustion (9.1 ng m^{-3}, 50.6%) and biomass burning (7.8 ng m^{-3}, 43.7%) were comparable
390 and vehicle emission (1.0 ng m^{-3}, 5.7%) had minor contributions. The major sources of
391 $\sum_{24}$PAHs varied among different size particles in the northern and southern China (Figure 7c).
392 For $PM_{>3.3}$-bound PAHs, the contributions of coal combustion (50.3%) and biomass burning
393 (48.4%) were comparable in the northern China, while biomass burning (71.0%) was the largest
394 source in the southern China. For $PM_{1.1\text{-}3.3}$-bound PAHs, coal combustion (66.7%) was the
395 dominated source in the northern China, whereas the percentage of biomass burning (53.7%)
396 was larger than that of coal combustion (40.4%) in the southern China. For $PM_{1.1}$-bound PAHs,
397 coal combustion was the dominated source in the northern (66.6%) and southern (59.3%) China.

398 Source apportionment of BaP_{eq} in different regions (Figure 7d), sampling sites (Figure 7e)
399 and size particles (Figure 7f) were also discussed. Unlike $\sum_{24}$PAHs, coal combustion was the
400 predominant source of BaP_{eq} in the northern (8.1 ng m^{-3} and 95.7%) and the southern (1.1 ng

401 m^{-3} and 84.7%) China. The contributions of coal contribution at urban sites (8.3 ng m^{-3} and
402 96.4%) were larger than those at sub-urban (3.3 ng m^{-3} and 90.8%) and remote (1.0 ng m^{-3} and
403 82.5%) sites. Coal combustion was the dominate source in different size particles. And its
404 contributions to $PM_{>3.3}$, $PM_{1.1\text{-}3.3}$ and $PM_{1.1}$-bound PAHs in the northern China (87.3%, 95.6%
405 and 96.9%) were all larger than those in the southern China (76.8%, 87.3% and 88.2%). Here,
406 we concluded that the unfavorable meteorological conditions and intensive emission especially
407 in coal combustion together led to severe PAHs pollution and high cancer risk in the atmosphere
408 of the northern China.

409 **3.4 Nationwide increase of PAHs pollution and health risk during winter**

410 Figure 8 exhibits monthly variations of BaP_{eq} and ILCR at the 12 sites. BaP_{eq} levels were
411 the highest in winter and the lowest in summer at all sites. As Figure 8 showed, the enhancement
412 of BaP_{eq} from summer to winter ranged from 1.05 (SY) to 32.5 (SPT). And such an
413 enhancement was much more significant at the northern sites than the southern sites. Hence,
414 ILCR was significantly enhanced in winter, especially in the northern China (Figure 8) and was
415 much higher than the acceptable risk level of 1.0×10^{-6} in US (USEPA, 1991). Previous studies
416 in different cities of China also reported such a winter-high trend of atmospheric PAHs (Liu et
417 al., 2017b; Ma et al., 2018; Shen et al., 2019). Thus, there is a nationwide increase of PAHs
418 pollution during winter in China.

419 The winter-high feature of PAHs pollution should result from the impacts of
420 meteorological conditions and source emissions. The winter to summer ratios of PAHs
421 correlated well with that for temperature (Figure S15). And T, SR and BLH were all the lowest
422 during winter and the highest during summer (Table S5-7). Coupled with the negative

correlations between PAHs and meteorological factors (Figure 4), the unfavorable meteorological conditions in wintertime did account for the increase in PAHs pollution.

Moreover, PAHs emitted from coal combustion and biomass burning apparently elevated during fall-winter (Figure 9). In the northern China, central heating systems in urban areas usually start from November to next March. Meanwhile residential heating in the rural areas of northern China consumes substantial coal and biofuel (Xue et al., 2016). Thus, the energy consumption in the residential sector is dramatically enhanced during fall-winter (Xue et al., 2016). In the southern China, although there is no central heating system in urban areas, power plant and industry consume large amounts of coal. And there is also residential coal/biofuel consumption for heating during winter as well as cooking in rural areas (Zhang et al., 2013; Xu et al., 2015). In addition, open burning of agriculture residuals which accounts for a major fraction of the total biomass burning in China will significantly increase during fall-winter harvest seasons in the southern China (Zhang et al., 2013). Our observation and emissions inventory witnessed similar monthly trends that the PAHs from solid fuel combustion (coal and biomass) apparently elevated during fall-winter in the northern and southern China (Figure S16). Previous field studies also found that the contributions of coal combustion and biomass burning to PAHs elevated during fall-winter (Lin et al., 2015a; Yu et al., 2016). Thus, we concluded that the unfavorable meteorological conditions and intensive source emission together led to the increase of PAHs pollution during winter.

Data availability

The data are given in the Supplement.

Author contributions

Qingqing Yu analyzed the data, wrote the paper and performed data interpretation. Quanfu He and Ruqin Shen analyzed the samples. Weiqiang Yang ran the PMF model and helped with the interpretation. Ming Zhu, Sheng Li and Runqi Zhang provided the meteorological data and prepared the related interpretation. Yanli Zhang and Xinhui Bi gave many suggestions about the results and discussion. Yuesi Wang helped the field observation and performed data interpretation. Xiang Ding, Ping'an Peng and Xinming Wang performed data interpretation, reviewed and edited this paper.

Competing interests

The authors declare that they have no conflict of interest.

Acknowledgement

This study was funded by the National Natural Science Foundation of China (41530641/4191101024/41722305/41907196), the National Key Research and Development Program (2016YFC0202204/2018YFC0213902), the Chinese Academy of Sciences (XDA05100104/QYZDJ-SSW-DQC032), and Guangdong Foundation for Science and Technology Research (2019B121205006/2017BT01Z134/ 2020B1212060053).

References

Aceves, M., Grimalt, J.O., 1993. Seasonally dependent size distributions of aliphatic and polycyclic aromatic hydrocarbons in urban aerosols from densely populated areas. Environ. Sci. Technol. 27, 2896-2908.

Armstrong, B., Hutchinson, E., Unwin, J., Fletcher, T., 2004. Lung cancer risk after exposure to polycyclic aromatic hydrocarbons: A review and meta-analysis. Environ. Health. Persp. 112, 970-978.

Belis, C.A., Cancelinha, J., Duane, M., Forcina, V., Pedroni, V., Passarella, R., Tanet, G., Douglas, K., Piazzalunga, A., Bolzacchini, E., Sangiorgi, G., Perrone, M.G., Ferrero, L., Fermo, P., Larsen, B.R., 2011. Sources for PM air pollution in the Po Plain, Italy: I. Critical comparison of methods for estimating biomass burning contributions to benzo(a)pyrene. Atmos. Environ. 45, 7266-7275.

Bi, X.H., Sheng, G.Y., Peng, P.A., Chen, Y.J., Zhang, Z.Q., Fu, J.M., 2003. Distribution of particulate- and vapor-phase n-alkanes and polycyclic aromatic hydrocarbons in urban atmosphere of Guangzhou, China. Atmos. Environ. 37, 289-298.

Brown, A.S., Brown, R.J.C., Coleman, P.J., Conolly, C., Sweetman, A.J., Jones, K.C., Butterfield, D.M., Sarantaridis, D., Donovan, B.J., Roberts, I., 2013. Twenty years of measurement of polycyclic aromatic hydrocarbons (PAHs) in UK ambient air by nationwide air quality networks. Environ. Sci.-Proc. Imp. 15, 1199-1215.

Callén, M.S., Iturmendi, A., López, J.M., 2014. Source apportionment of atmospheric $PM_{2.5}$-bound polycyclic aromatic hydrocarbons by a PMF receptor model. Assessment of potential risk for human health. Environ. Pollut. 195, 167-177.

Cass, G.R., 1998. Organic molecular tracers for particulate air pollution sources. Trac.-Trend Anal. Chem. 17, 356-366.

Chung, Y., Dominici, F., Wang, Y., Coull, B.A., Bell, M.L., 2015. Associations between long-term exposure to chemical constituents of fine particulate matter ($PM_{2.5}$) and mortality in medicare enrollees in the eastern United States. Environ. Health Persp. 123, 467-474.

Cohen, A.J., Brauer, M., Burnett, R., Anderson, H.R., Frostad, J., Estep, K., Balakrishnan, K., Brunekreef, B., Dandona, L., Dandona, R., Feigin, V., Freedman, G., Hubbell, B., Jobling, A., Kan, H., Knibbs, L., Liu, Y., Martin, R., Morawska, L., Pope, C.A., Shin, H., Straif, K., Shaddick, G., Thomas, M., van Dingenen, R., van Donkelaar, A., Vos, T., Murray, C.J.L., Forouzanfar, M.H., 2017. Estimates and 25-year trends of the global burden of disease attributable to ambient air pollution: An analysis of data from the Global Burden of Diseases Study 2015. Lancet 389, 1907-1918.

Dai, S., Bi, X., Chan, L.Y., He, J., Wang, B., Wang, X., Peng, P., Sheng, G., Fu, J., 2015. Chemical and stable carbon isotopic composition of $PM_{2.5}$ from on-road vehicle emissions in the PRD region and implications for vehicle emission control policy. Atmos. Chem. Phys. 15, 3097-3108.

Ding, X., He, Q.F., Shen, R.Q., Yu, Q.Q., Wang, X.M., 2014. Spatial distributions of secondary organic aerosols from isoprene, monoterpenes, beta-caryophyllene, and aromatics over China during summer. J. Geophys. Res.-Atmos. 119, 11877-11891.

Ding, X., Wang, X.M., Xie, Z.Q., Xiang, C.H., Mai, B.X., Sun, L.G., Zheng, M., Sheng, G.Y., Fu, J.M., Poschl, U., 2007. Atmospheric polycyclic aromatic hydrocarbons observed over the North Pacific Ocean and the Arctic area: Spatial distribution and source identification.

505 Atmos. Environ. 41, 2061-2072.

506 Dong, W., Pan, L., Li, H., Miller, M.R., Loh, M., Wu, S., Xu, J., Yang, X., Shan, J., Chen, Y.,
507 Deng, F., Guo, X., 2018. Association of size-fractionated indoor particulate matter and
508 black carbon with heart rate variability in healthy elderly women in Beijing. Indoor Air
509 28, 373-382.

510 Duan, J.C., Bi, X.H., Tan, J.H., Sheng, G.Y., Fu, J.M., 2007. Seasonal variation on size
511 distribution and concentration of PAHs in Guangzhou city, China. Chemosphere 67, 614-
512 622.

513 Gao, B., Guo, H., Wang, X.M., Zhao, X.Y., Ling, Z.H., Zhang, Z., Liu, T.Y., 2012. Polycyclic
514 aromatic hydrocarbons in $PM_{2.5}$ in Guangzhou, southern China: Spatiotemporal patterns
515 and emission sources. J. Hazard. Mater. 239, 78-87.

516 Gao, B., Guo, H., Wang, X.M., Zhao, X.Y., Ling, Z.H., Zhang, Z., Liu, T.Y., 2013. Tracer-based
517 source apportionment of polycyclic aromatic hydrocarbons in $PM_{2.5}$ in Guangzhou,
518 southern China, using positive matrix factorization (PMF). Environ. Sci. Pollut. R. 20,
519 2398-2409.

520 Gao, B., Wang, X.M., Zhao, X.Y., Ding, X., Fu, X.X., Zhang, Y.L., He, Q.F., Zhang, Z., Liu,
521 T.Y., Huang, Z.Z., Chen, L.G., Peng, Y., Guo, H., 2015. Source apportionment of
522 atmospheric PAHs and their toxicity using PMF: Impact of gas/particle partitioning.
523 Atmos. Environ. 103, 114-120.

524 Gao, B., Yu, J.Z., Li, S.X., Ding, X., He, Q.F., Wang, X.M., 2011. Roadside and rooftop
525 measurements of polycyclic aromatic hydrocarbons in $PM_{2.5}$ in urban Guangzhou:
526 Evaluation of vehicular and regional combustion source contributions. Atmos. Environ.

527 45, 7184-7191.
528 Garrido, A., Jiménez-Guerrero, P., Ratola, N., 2014. Levels, trends and health concerns of
529 atmospheric PAHs in Europe. Atmos. Environ. 99, 474-484.
530 Gu, Z.P., Feng, J.L., Han, W.L., Li, L., Wu, M.H., Fu, J.M., Sheng, G.Y., 2010. Diurnal
531 variations of polycyclic aromatic hydrocarbons associated with $PM_{2.5}$ in Shanghai, China.
532 J. Environ. Sci. 22, 389-396.
533 Guo, H., Lee, S.C., Ho, K.F., Wang, X.M., Zou, S.C., 2003. Particle-associated polycyclic
534 aromatic hydrocarbons in urban air of Hong Kong. Atmos. Environ. 37, 5307-5317.
535 Hayakawa, K., Tang, N., Nagato, E.G., Toriba, A., Sakai, S., Kano, F., Goto, S., Endo, O.,
536 Arashidani, K.-i., Kakimoto, H., 2018. Long term trends in atmospheric concentrations of
537 polycyclic aromatic hydrocarbons and nitropolycyclic aromatic hydrocarbons: A study of
538 Japanese cities from 1997 to 2014. Environ. Pollut. 233, 474-482.
539 He, J.B., Fan, S.X., Meng, Q.Z., Sun, Y., Zhang, J., Zu, F., 2014. Polycyclic aromatic
540 hydrocarbons (PAHs) associated with fine particulate matters in Nanjing, China:
541 Distributions, sources and meteorological influences. Atmos. Environ. 89, 207-215.
542 Hong, W.J., Jia, H.L., Ma, W.L., Sinha, R.K., Moon, H.-B., Nakata, H., Minh, N.H., Chi, K.H.,
543 Li, W.L., Kannan, K., Sverko, E., Li, Y.F., 2016. Distribution, fate, inhalation exposure
544 and lung cancer risk of atmospheric polycyclic aromatic hydrocarbons in aome Asian
545 countries. Environ. Sci. Technol. 13, 7163-7174.
546 Huang, X.F., He, L.Y., Hu, M., Zhang, Y.H., 2006. Annual variation of particulate organic
547 compounds in $PM_{2.5}$ in the urban atmosphere of Beijing. Atmos. Environ. 40, 2449-2458.
548 Inomata, Y., Kajino, M., Sato, K., Ohara, T., Kurokawa, J. I., Ueda, H., Tang, N., Hayakawa,

549 K., Ohizumi, T., Akimoto, H., 2012. Emission and atmospheric transport of particulate
550 PAHs in Northeast Asia. Environ. Sci. Technol. 46, 4941-4949.
551 International Agency for Research on Cancer, 2001. Overall Evaluations of Carcinogenicity to
552 Humans.
553 Jaward, F.M., Farrar, N.J., Harner, T., Sweetman, A.J., Jones, K.C., 2004. Passive air sampling
554 of polycyclic aromatic hydrocarbons and polychlorinated naphthalenes across Europe.
555 Environ. Toxicol. Chem. 23, 1355-1364.
556 John, K., Ragavan, N., Pratt, M.M., Singh, P.B., Al-Buheissi, S., Matanhelia, S.S., Phillips,
557 D.H., Poirier, M.C., Martin, F.L., 2009. Quantification of phase I/II metabolizing enzyme
558 gene expression and polycyclic aromatic hydrocarbon–DNA adduct levels in human
559 prostate. The Prostate 69, 505-519.
560 Kim, K.H., Jahan, S.A., Kabir, E., Brown, R.J.C., 2013. A review of airborne polycyclic
561 aromatic hydrocarbons (PAHs) and their human health effects. Environ. Int. 60, 71-80.
562 Kuo, C.Y., Hsu, Y.W., Lee, H.S., 2003. Study of human exposure to particulate PAHs using
563 personal air samplers. Arch. Environ. Con. Tox. 44, 0454-0459.
564 Lang, C., Tao, S., Wang, X.J., Zhang, G., Li, J., Fu, J.M., 2007. Seasonal variation of polycyclic
565 aromatic hydrocarbons (PAHs) in Pearl River Delta region, China. Atmos. Environ. 41,
566 8370-8379.
567 Larsen, R.K., Baker, J.E., 2003. Source apportionment of polycyclic aromatic hydrocarbons in
568 the urban atmosphere: A comparison of three methods. Environ. Sci. Technol. 37, 1873-
569 1881.
570 Li, H.Y., Guo, L.L., Cao, R.F., Gao, B., Yan, Y.L., He, Q.S., 2016a. A wintertime study of $PM_{2.5}$-

571 bound polycyclic aromatic hydrocarbons in Taiyuan during 2009-2013: Assessment of
572 pollution control strategy in a typical basin region. Atmos. Environ. 140, 404-414.
573 Li, H., Li, H., Zhang, L., Cheng, M., Guo, L., He, Q., Wang, X., Wang, Y., 2019. High cancer
574 risk from inhalation exposure to PAHs in Fenhe Plain in winter: A particulate size
575 distribution-based study. Atmos. Environ. 216, 116924.
576 Li, J., Zhang, G., Li, X.D., Qi, S.H., Liu, G.Q., Peng, X.Z., 2006. Source seasonality of
577 polycyclic aromatic hydrocarbons (PAHs) in a subtropical city, Guangzhou, South China.
578 Sci. Total Environ. 355, 145-155.
579 Li, X., Yang, Y., Xu, X., Xu, C., Hong, J., 2016b. Air pollution from polycyclic aromatic
580 hydrocarbons generated by human activities and their health effects in China. J. Clean
581 Prod. 112, 1360-1367.
582 Lin, Y., Ma, Y.Q., Qiu, X.H., Li, R., Fang, Y.H., Wang, J.X., Zhu, Y.F., Hu, D., 2015a. Sources,
583 transformation, and health implications of PAHs and their nitrated, hydroxylated, and
584 oxygenated derivatives in $PM_{2.5}$ in Beijing. J. Geophys. Res.- Atmos. 120, 7219-7228.
585 Lin, Y., Qiu, X.H., Ma, Y.Q., Ma, J., Zheng, M., Shao, M., 2015b. Concentrations and spatial
586 distribution of polycyclic aromatic hydrocarbons (PAHs) and nitrated PAHs (NPAHs) in
587 the atmosphere of North China, and the transformation from PAHs to NPAHs. Environ.
588 Pollut. 196, 164-170.
589 Liu, B., Xue, Z., Zhu, X., Jia, C., 2017a. Long-term trends (1990–2014), health risks, and
590 sources of atmospheric polycyclic aromatic hydrocarbons (PAHs) in the U.S. Environ.
591 Pollut. 220, 1171-1179.
592 Liu, D., Lin, T., Syed, J.H., Cheng, Z.N., Xu, Y., Li, K.C., Zhang, G., Li, J., 2017b.

593 Concentration, source identification, and exposure risk assessment of $PM_{2.5}$-bound parent
594 PAHs and nitro-PAHs in atmosphere from typical Chinese cities. Sci. Rep.-UK. 7, 10398.
595 Liu, S.Z., Tao, S., Liu, W.X., Dou, H., Liu, Y.N., Zhao, J.Y., Little, M.G., Tian, Z.F., Wang, J.F.,
596 Wang, L.G., Gao, Y., 2008. Seasonal and spatial occurrence and distribution of
597 atmospheric polycyclic aromatic hydrocarbons (PAHs) in rural and urban areas of the
598 North Chinese Plain. Environ. Pollut. 156, 651-656.
599 Liu, S.Z., Tao, S., Liu, W.X., Liu, Y.N., Dou, H., Zhao, J.Y., Wang, L.G., Wang, J.F., Tian, Z.F.,
600 Gao, Y., 2007a. Atmospheric polycyclic aromatic hydrocarbons in north China: A winter-
601 time study. Environ. Sci. Technol. 41, 8256-8261.
602 Liu, X., Zhang, G., Li, J., Cheng, H.R., Qi, S.H., Li, X.D., Jones, K.C., 2007b. Polycyclic
603 aromatic hydrocarbons (PAHs) in the air of Chinese cities. J. Environ. Monitor. 9, 1092-
604 1098.
605 Liu, Y.J., Zhu, L.Z., Shen, X.Y., 2001. Polycyclic aromatic hydrocarbons (PAHs) in indoor and
606 outdoor air of Hangzhou, China. Environ. Sci. Technol. 35, 840-844.
607 Lv, Y., Li, X., Xu, T.T., Cheng, T.T., Yang, X., Chen, J.M., Iinuma, Y., Herrmann, H., 2016.
608 Size distributions of polycyclic aromatic hydrocarbons in urban atmosphere: Sorption
609 mechanism and source contributions to respiratory deposition. Atmos. Chem. Phys. 16,
610 2971-2983.
611 Ma, W.L., Liu, L.Y., Jia, H.L., Yang, M., Li, Y.F., 2018. PAHs in Chinese atmosphere Part I:
612 Concentration, source and temperature dependence. Atmos. Environ. 173, 330-337.
613 Ma, W.L., Zhu, F.J., Hu, P.T., Qiao, L.N., Li, Y.F., 2020. Gas/particle partitioning of PAHs based
614 on equilibrium-state model and steady-state model. Sci. Total Environ. 706. 136029.

615 Mastral, A.M., Callén, M.S., 2000. A review on polycyclic aromatic hydrocarbon (PAH)
616 emissions from energy generation. Environ. Sci. Technol. 34, 3051-3057.
617 Nisbet, I.C.T., Lagoy, P.K., 1992. Toxic equivalency factors (TEFs) for polycyclic aromatic
618 hydrocarbons (PAHs). Regul. Toxicol. Pharm. 16, 290-300.
619 Polissar, A.V., Hopke, P.K., Paatero, P., 1998. Atmospheric aerosol over Alaska 2. Elemental
620 composition and sources. J. Geophys. Res.- Atmos. 103, 19045-19057.
621 Shen, H.Z., Huang, Y., Wang, R., Zhu, D., Li, W., Shen, G.F., Wang, B., Zhang, Y.Y., Chen,
622 Y.C., Lu, Y., Chen, H., Li, T.C., Sun, K., Li, B.G., Liu, W.X., Liu, J.F., Tao, S., 2013a.
623 Global atmospheric emissions of polycyclic aromatic hydrocarbons from 1960 to 2008
624 and future predictions. Environ. Sci. Technol. 47, 6415-6424.
625 Shen, G.F., Tao, S., Chen, Y.C., Zhang, Y.Y., Wei, S.Y., Xue, M., Wang, B., Wang, R., Lu, Y.,
626 Li, W., Shen, H.Z., Huang, Y., Chen, H., 2013b. Emission characteristics for polycyclic
627 aromatic hydrocarbons from solid fuels burned in domestic stoves in rural China. Environ.
628 Sci. Technol. 47, 14485-14494.
629 Shen, R., Wang, Y., Gao, W., Cong, X., Cheng, L., Li, X., 2019. Size-segregated particulate
630 matter bound polycyclic aromatic hydrocarbons (PAHs) over China: Size distribution,
631 characteristics and health risk assessment. Sci. Total Environ. 685, 116-123.
632 Shrivastava, M., Lou, S., Zelenyuk, A., Easter, R.C., Corley, R.A., Thrall, B.D., Rasch, P.J.,
633 Fast, J.D., Massey Simonich, S.L., Shen, H., Tao, S., 2017. Global long-range transport
634 and lung cancer risk from polycyclic aromatic hydrocarbons shielded by coatings of
635 organic aerosol. P. Natl. Acad. Sci. USA 114, 1246-1251.
636 Sofuoglu, A., Odabasi, M., Tasdemir, Y., Khalili, N.R., Holsen, T.M., 2001. Temperature

637 dependence of gas-phase polycyclic aromatic hydrocarbon and organochlorine pesticide
638 concentrations in Chicago air. Atmos. Environ. 35, 6503-6510.
639 Song, C.B., He, J.J., Wu, L., Jin, T.S., Chen, X., Li, R.P., Ren, P.P., Zhang, L., Mao, H.J., 2017.
640 Health burden attributable to ambient $PM_{2.5}$ in China. Environ. Pollut. 223, 575-586.
641 Sun, P., Blanchard, P., Brice, K.A., Hites, R.A., 2006. Trends in polycyclic aromatic
642 hydrocarbon concentrations in the Great Lakes atmosphere. Environ. Sci. Technol. 40,
643 6221-6227.
644 Tan, J.H., Bi, X.H., Duan, J.C., Rahn, K.A., Sheng, G.Y., Fu, J.M., 2006. Seasonal variation of
645 particulate polycyclic aromatic hydrocarbons associated with PM_{10} in Guangzhou, China.
646 Atmos. Res. 80, 250-262.
647 Tang, N., Suzuki, G., Morisaki, H., Tokuda, T., Yang, X.Y., Zhao, L.X., Lin, J.M., Kameda, T.,
648 Toriba, A., Hayakawa, K., 2017. Atmospheric behaviors of particulate-bound polycyclic
649 aromatic hydrocarbons and nitropolycyclic aromatic hydrocarbons in Beijing, China from
650 2004 to 2010. Atmos. Environ. 152, 354-361.
651 USEPA, 1991. Role of the baseline risk assessment in Superfund remedy-selection decisions.
652 Office of Solid Waste and Emergency Response, Washington.
653 Wang, G., Kawamura, K., Lee, S., Ho, K., Cao, J., 2006. Molecular, seasonal, and spatial
654 distributions of organic aerosols from fourteen Chinese cities. Environ. Sci. Technol. 40,
655 4619-4625.
656 Wang, G., Kawamura, K., Xie, M., Hu, S., Gao, S., Cao, J., An, Z., Wang, Z., 2009. Size-
657 distributions of n-alkanes, PAHs and hopanes and their sources in the urban, mountain and
658 marine atmospheres over East Asia. Atmos. Chem. Phys. 9, 8869-8882.

659 Wang, Q.Y., Kobayashi, K., Lu, S.L., Nakajima, D., Wang, W.Q., Zhang, W.C., Sekiguchi, K.,
660 Terasaki, M., 2016. Studies on size distribution and health risk of 37 species of polycyclic
661 aromatic hydrocarbons associated with fine particulate matter collected in the atmosphere
662 of a suburban area of Shanghai city, China. Environ. Pollut. 214, 149-160.
663 Wang, W.T., Simonich, S.L.M., Wang, W., Giri, B., Zhao, J.Y., Xue, M., Cao, J., Lu, X.X., Tao,
664 S., 2011. Atmospheric polycyclic aromatic hydrocarbon concentrations and gas/particle
665 partitioning at background, rural village and urban sites in the North China Plain. Atmos.
666 Res. 99, 197-206.
667 World Health Organization (WHO), 2000. Air Quality Guidelines for Europe, 2nd Edition,
668 World Health Organization Regional Office for Europe, Copenhagen.
669 Xu, H.J., Wang, X.M., Poesch, U., Feng, S.L., Wu, D., Yang, L., Li, S.X., Song, W., Sheng,
670 G.Y., Fu, J.M., 2008. Genotoxicity of total and fractionated extractable organic matter in
671 fine air particulate matter from urban Guangzhou: Comparison between haze and nonhaze
672 episodes. Environ. Toxicol. Chem. 27, 206-212.
673 Xu, J., Chang, S.Y., Yuan, Z.H., Jiang, Y., Liu, S.N., Li, W.Z., Ma, L.L., 2015. Regionalized
674 techno-economic assessment and policy analysis for biomass molded fuel in China.
675 Energies 8, 13846-13863.
676 Xu, S.S., Liu, W.X., Tao, S., 2006. Emission of polycyclic aromatic hydrocarbons in China.
677 Environ. Sci. Technol. 40, 702-708.
678 Xue, Y.F., Zhou, Z., Nie, T., Wang, K., Nie, L., Pan, T., Wu, X.Q., Tian, H.Z., Zhong, L.H., Li,
679 J., Liu, H.J., Liu, S.H., Shao, P.Y., 2016. Trends of multiple air pollutants emissions from
680 residential coal combustion in Beijing and its implication on improving air quality for

control measures. Atmos. Environ. 142, 303-312.

Yang, G.H., Wang, Y., Zeng, Y.X., Gao, G.F., Liang, X.F., Zhou, M.G., Wan, X., Yu, S.C., Jiang, Y.H., Naghavi, M., Vos, T., Wang, H.D., Lopez, A.D., Murray, C.J.L., 2013. Rapid health transition in China, 1990-2010: Findings from the Global Burden of Disease Study 2010. Lancet 381, 1987-2015.

Yang, Y.Y., Guo, P.R., Zhang, Q., Li, D.L., Zhao, L., Mu, D.H., 2010. Seasonal variation, sources and gas/particle partitioning of polycyclic aromatic hydrocarbons in Guangzhou, China. Sci. Total Environ. 408, 2492-2500.

Yin, P., Guo, J., Wang, L., Fan, W., Lu, F., Guo, M., Moreno, S.B.R., Wang, Y., Wang, H., Zhou, M., Dong, Z., 2020. Higher risk of cardiovascular disease associated with smaller size-fractioned particulate matter. Environ. Sci. Technol. Let. 7, 95-101.

Yu, Q.Q., Gao, B., Li, G.H., Zhang, Y.L., He, Q.F., Deng, W., Huang, Z.H., Ding, X., Hu, Q.H., Huang, Z.Z., Wang, Y.J., Bi, X.H., Wang, X.M., 2016. Attributing risk burden of $PM_{2.5}$-bound polycyclic aromatic hydrocarbons to major emission sources: Case study in Guangzhou, south China. Atmos. Environ. 142, 313-323.

Yu, Q.Q., Yang, W.Q., Zhu, M., Gao, B., Li, S., Li, G.H., Fang, H., Zhou, H.S., Zhang, H.N., Wu, Z.F., Song, W., Tan, J.H., Zhang, Y.L., Bi, X.H., Chen, L.G., Wang, X.M., 2018. Ambient $PM_{2.5}$-bound polycyclic aromatic hydrocarbons (PAHs) in rural Beijing: Unabated with enhanced temporary emission control during the 2014 APEC summit and largely aggravated after the start of wintertime heating. Environ. Pollut. 238, 532-542.

Yu, Y.X., Li, Q., Wang, H., Wang, B., Wang, X.L., Ren, A.G., Tao, S., 2015. Risk of human exposure to polycyclic aromatic hydrocarbons: A case study in Beijing, China. Environ.

703 Pollut. 205, 70-77.
704 Yunker, M.B., Macdonald, R.W., Vingarzan, R., Mitchell, R.H., Goyette, D., Sylvestre, S., 2002.
705 PAHs in the Fraser River basin: A critical appraisal of PAH ratios as indicators of PAH
706 source and composition. Org. Geochem. 33, 489-515.
707 Zelenyuk, A., Imre, D., Beranek, J., Abramson, E., Wilson, J., Shrivastava, M., 2012. Synergy
708 between secondary organic aerosols and long-range transport of polycyclic aromatic
709 hydrocarbons. Environ. Sci. Technol. 46, 12459-12466.
710 Zhang, K., Zhang, B.Z., Li, S.M., Wong, C.S., Zeng, E.Y., 2012. Calculated respiratory
711 exposure to indoor size-fractioned polycyclic aromatic hydrocarbons in an urban
712 environment. Sci. Total Environ. 431, 245-251.
713 Zhang, Y.S., Shao, M., Lin, Y., Luan, S.J., Mao, N., Chen, W.T., Wang, M., 2013. Emission
714 inventory of carbonaceous pollutants from biomass burning in the Pearl River Delta
715 Region, China. Atmos. Environ. 76, 189-199.
716 Zhang, X.L., Tao, S., Liu, W.X., Yang, Y., Zuo, Q., Liu, S.Z., 2005. Source diagnostics of
717 polycyclic aromatic hydrocarbons based on species ratios: A multimedia approach.
718 Environ. Sci. Technol. 39, 9109-9114.
719 Zhang, Y.X., Tao, S., 2008. Seasonal variation of polycyclic aromatic hydrocarbons (PAHs)
720 emissions in China. Environ. Pollut. 156, 657-663.
721 Zhang, Y.X., Tao, S., 2009. Global atmospheric emission inventory of polycyclic aromatic
722 hydrocarbons (PAHs) for 2004. Atmos. Environ. 43, 812-819.
723 Zhang, Y.X., Tao, S., Cao, J., Coveney, R.M., 2007. Emission of polycyclic aromatic
724 hydrocarbons in China by county. Environ. Sci. Technol. 41, 683-687.

Zhang, Y., Shen, H., Tao, S., Ma, J., 2011. Modeling the atmospheric transport and outflow of polycyclic aromatic hydrocarbons emitted from China. Atmos. Environ. 45, 2820-2827.

Zhang, Y.X., Tao, S., Shen, H.Z., Ma, J.M., 2009. Inhalation exposure to ambient polycyclic aromatic hydrocarbons and lung cancer risk of Chinese population. P. Natl. Acad. Sci. USA 106, 21063-21067.

Zhu, L.Z., Lu, H., Chen, S.G., Amagai, T., 2009. Pollution level, phase distribution and source analysis of polycyclic aromatic hydrocarbons in residential air in Hangzhou, China. J. Hazard. Mater. 162, 1165-1170.

Zhu, Y., Tao, S., Price, O.R., Shen, H.Z., Jones, K.C., Sweetman, A.J., 2015. Environmental distributions of benzo[a]pyrene in China: Current and future emission reduction scenarios explored using a spatially explicit multimedia fate model. Environ. Sci. Technol. 49, 13868-13877.

738 Table 1 PAHs concentration measured in this study and comparison with those of other large scale
739 observations.

Site/type	Sampling period	Sample type	# of sites	# of species	PAHs (ng/m^3)	Reference
China[a]	Oct, 2012-Sep, 2013	$PM_{1.1}$	12	24	3.4-126.2	This study
China[a]	Oct, 2012-Sep, 2013	$PM_{1.1-3.3}$	12	24	2.4-55.7	This study
China[a]	Oct, 2012-Sep, 2013	$PM_{>3.3}$	12	24	1.8-22.7	This study
China/Urban	2003	$PM_{2.5}$	14	18	1.7-701	Wang et al., 2006
China[b]	2005	PUF	40	20	374.5[e]	Liu et al., 2007
China/Urban	2013-2014	$PM_{2.5}$	9	16	14-210	Liu et al., 2017b
China/Urban	Aug, 2008-July, 2009	$PM_{2.5}$	11	16	75.4-478	Ma et al., 2018
China[c]	Jan, 2013-Dec, 2014	$PM_{9.0}$[e]	10	12	17.3-244.3	Shen et al., 2019
Great Lakes	1996-2003	PUF	7	16	0.59-70	Sun et al., 2006
Asian countries[d]	Sep, 2012-Aug, 2013	PUF	176	47	6.29-688	Hong et al., 2016
U.S.	1990-2014	PUF	169	15	52.6	Liu et al., 2017a
Japan	1997-2014	TSP	5	9	0.21-3.73	Hayakawa et al., 2018
Europe	2002	PUF	22	12	0.5-61.2	Jaward et al., 2004

740 a: including 5 urban sites, 3 sub-urban sites and 4 remote sites in China
741 b: including 37 cities and 3 rural locations in China
742 c: including 5 urban sites, 1 sub-urban site, 1 farmland site and 3 background sites in China
743 d: including 82 urban sites, 83 rural sites and 11 background sites in China, Japan, South Korea,
744 Vietnam, and India
745 e: the unit was ng/day
746

747 Table 2 Correlation coefficient (r), significance (p) of PAHs between paired sites in each region.

	Northern China			Southern China	
regions	north	northeast	northwest	east	southwest
paired sites	BJ-TY	HL-TYU	DH-SPT	WX-HF	KM-BN
distance between sites	400 km	450 km	940 km	280 km	380 km
r	0.97	0.80	0.63	0.77	-
p	<0.001	<0.001	0.001	<0.001	0.09

748

749

750

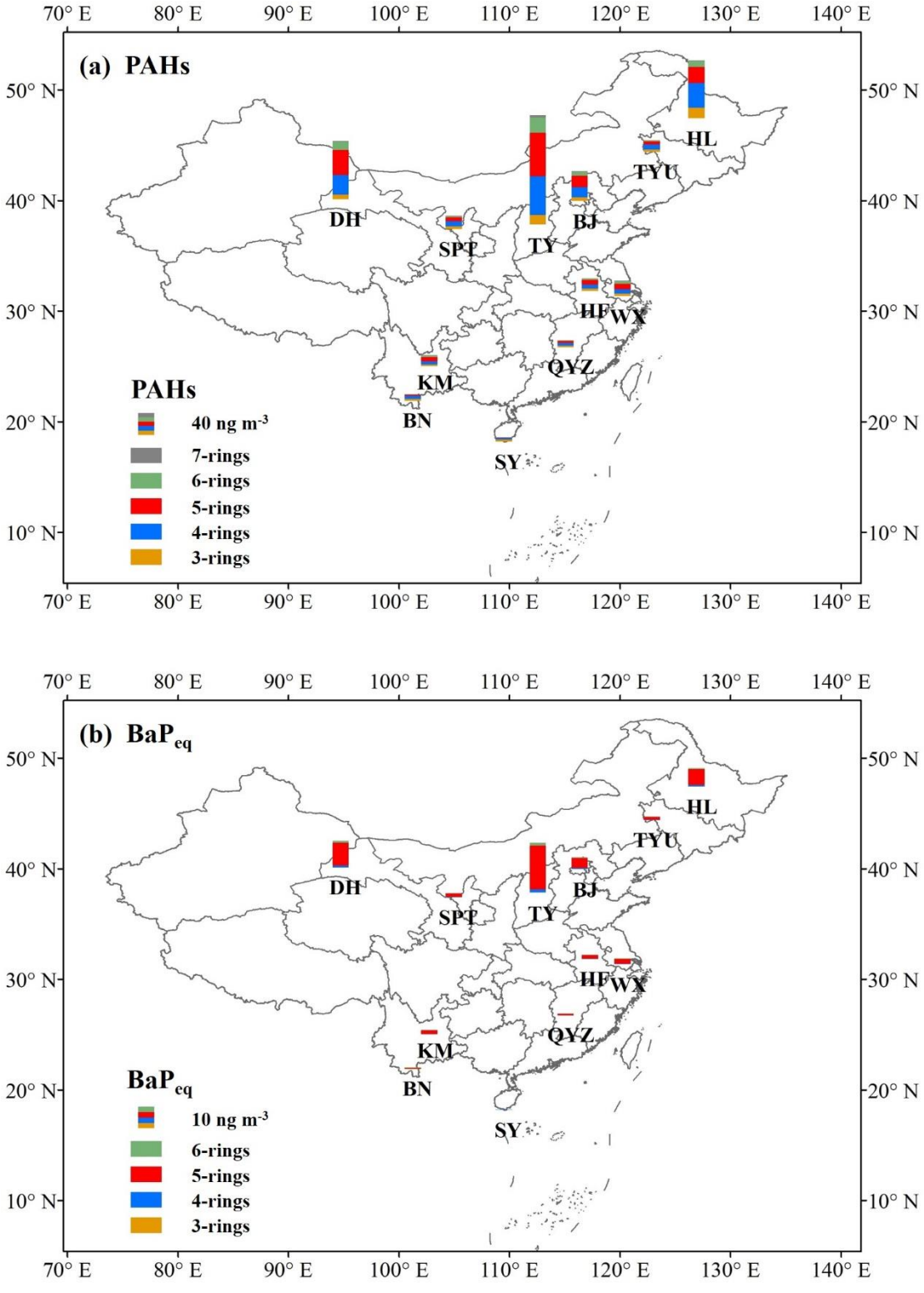

751

752 Figure 1 Annual averages of $\sum_{24}$PAHs (a) and BaP_{eq} (b) at 12 sites in China.

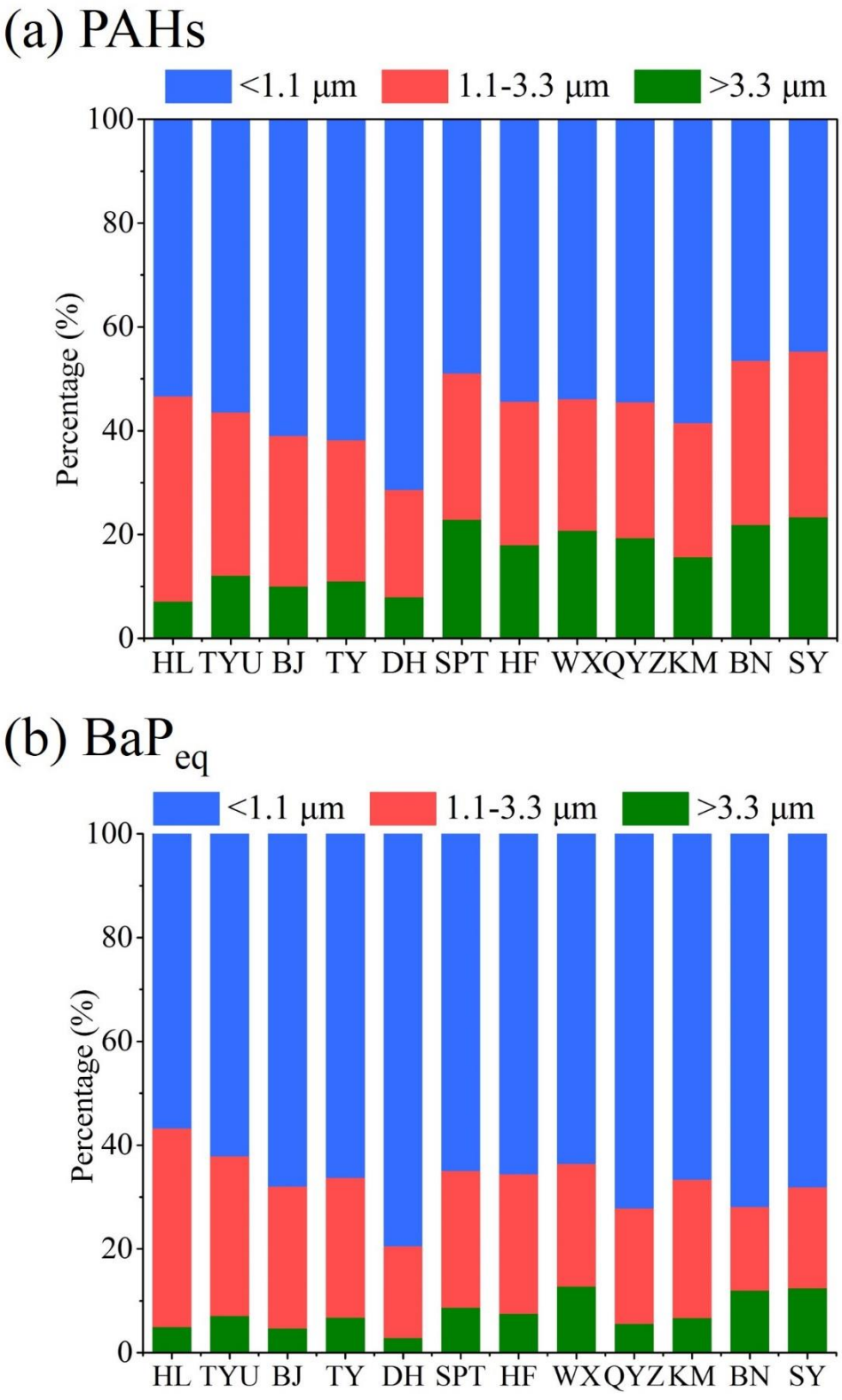

753

754 Figure 2 Size distribution of total measured PAHs (a) and BaP_{eq} (b) at 12 sites over China.

755

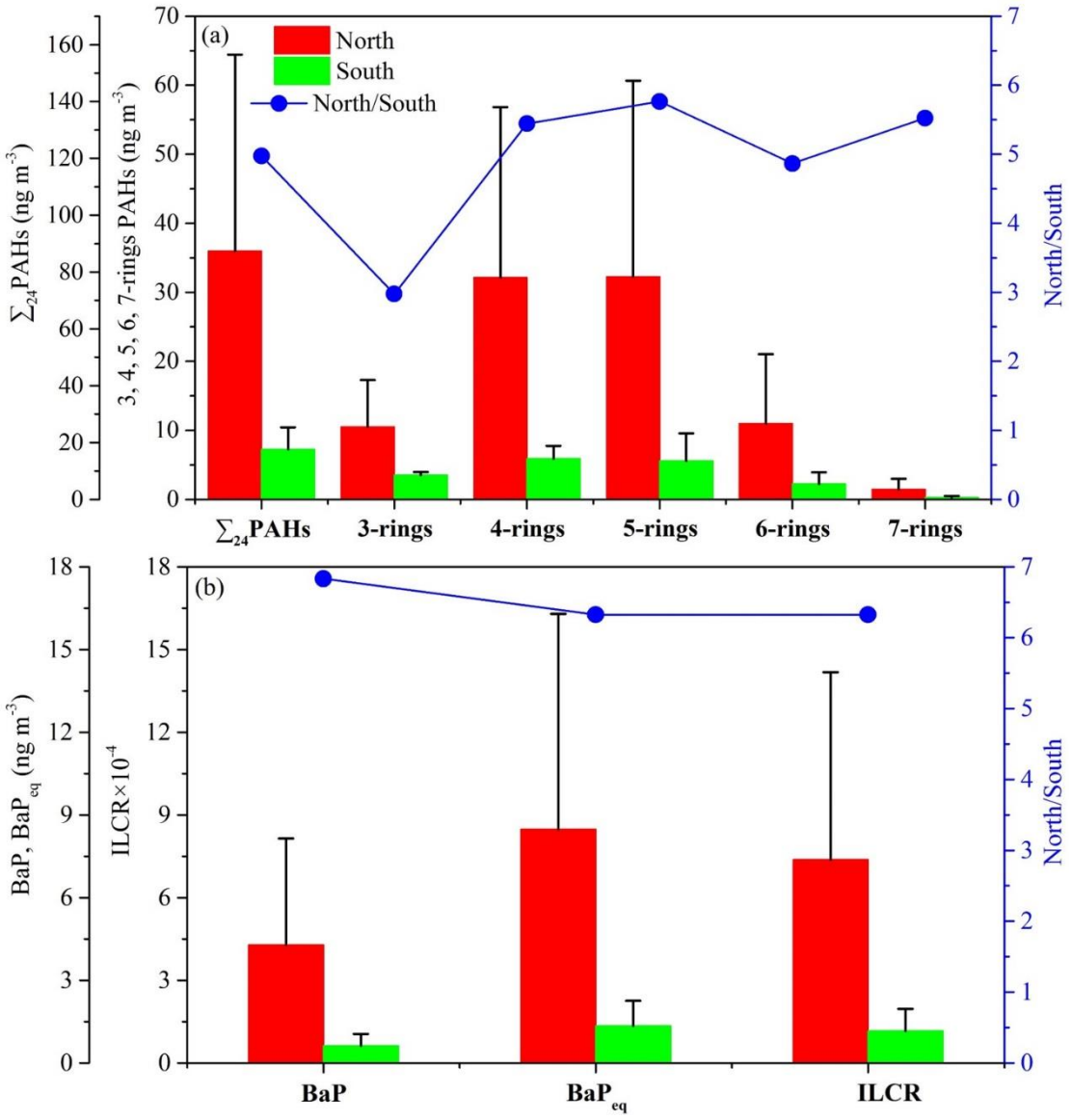

Figure 3 Comparison between the northern and the southern China in $\sum_{24}$PAHs, 3-7 rings PAHs (a) and BaP, BaP_{eq} and ILCR (b).

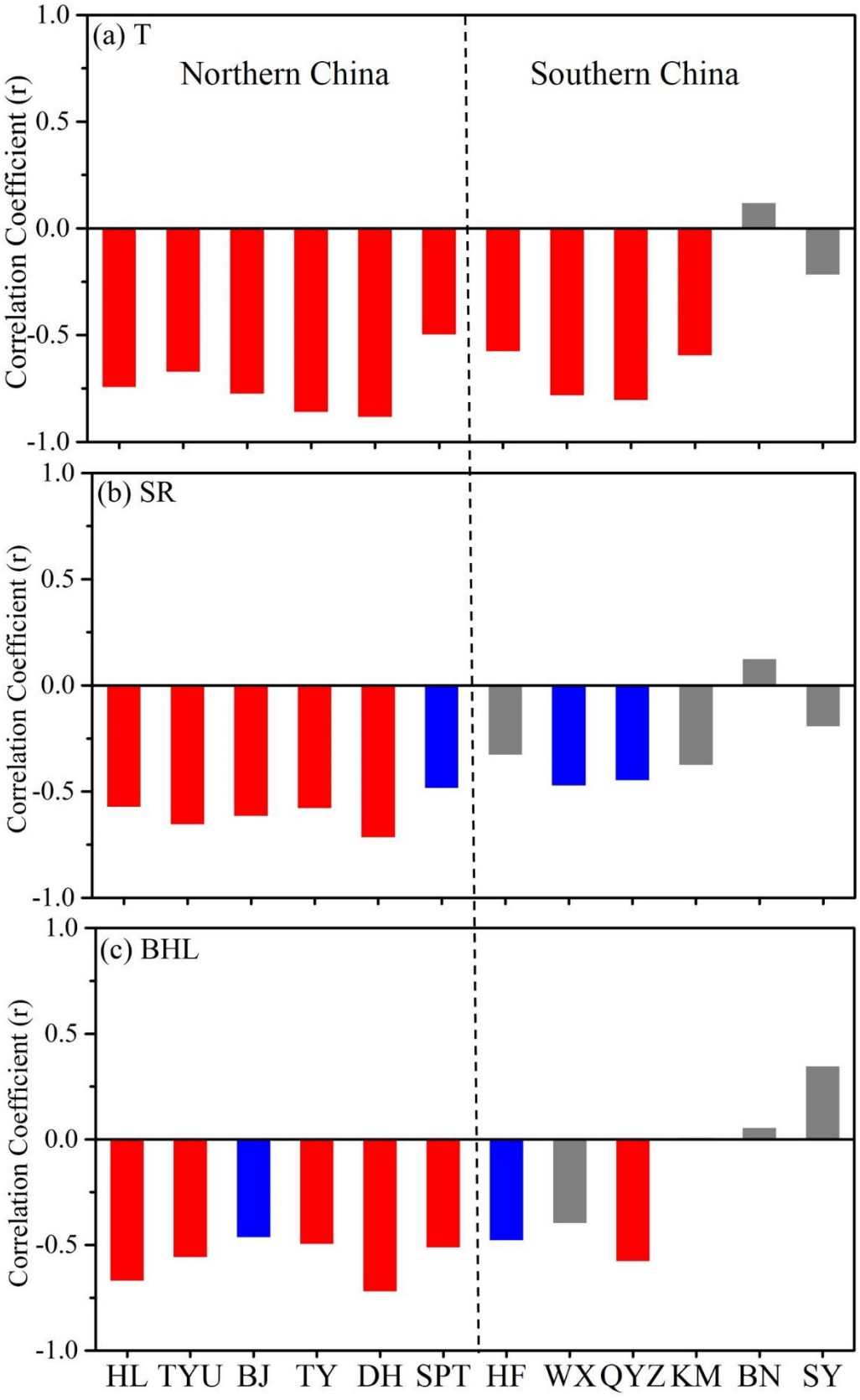

760

761 Figure 4 Correlation coefficient (r) of PAHs with T (a), SR (b) and BLH (c) at 12 sites. The

762 red, blue and gray bars indicate $p<0.01$, $p<0.05$ and $p>0.05$, respectively.

763

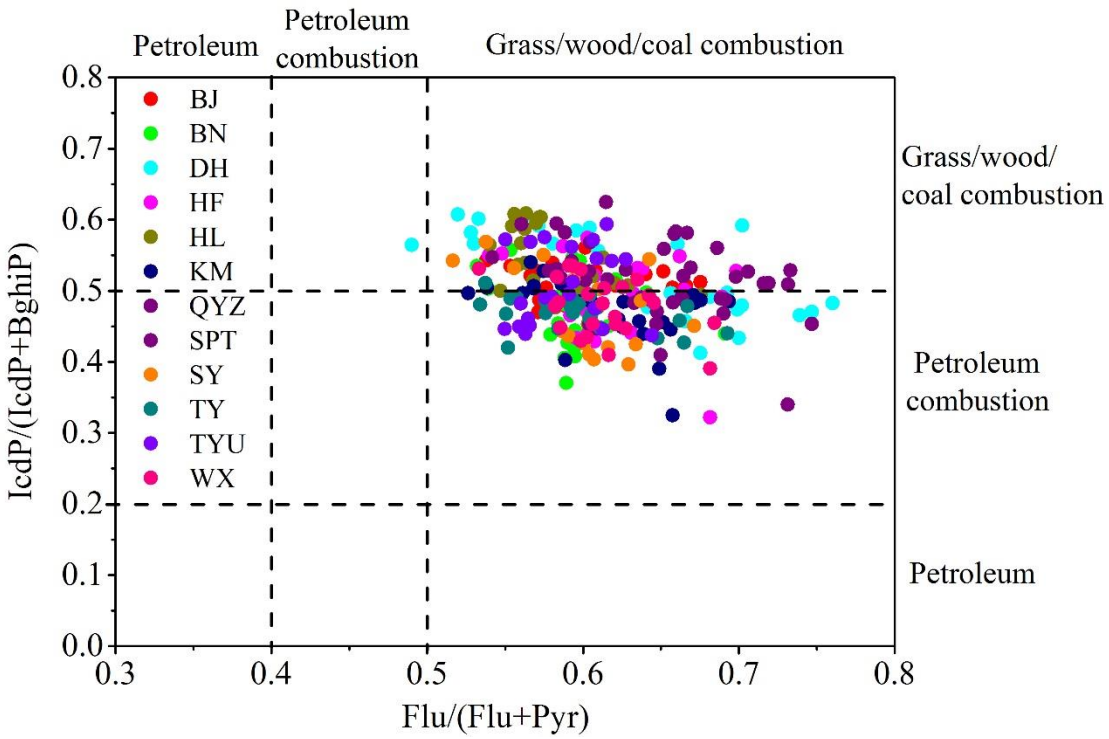

764

765 Figure 5 Diagnostic ratios of IcdP/(IcdP +BgiP) versus Flu/(Flu+Pyr) at 12 sites in China.

766 Ranges of ratios for sources are adopted from Yunker et al. (2002).

767

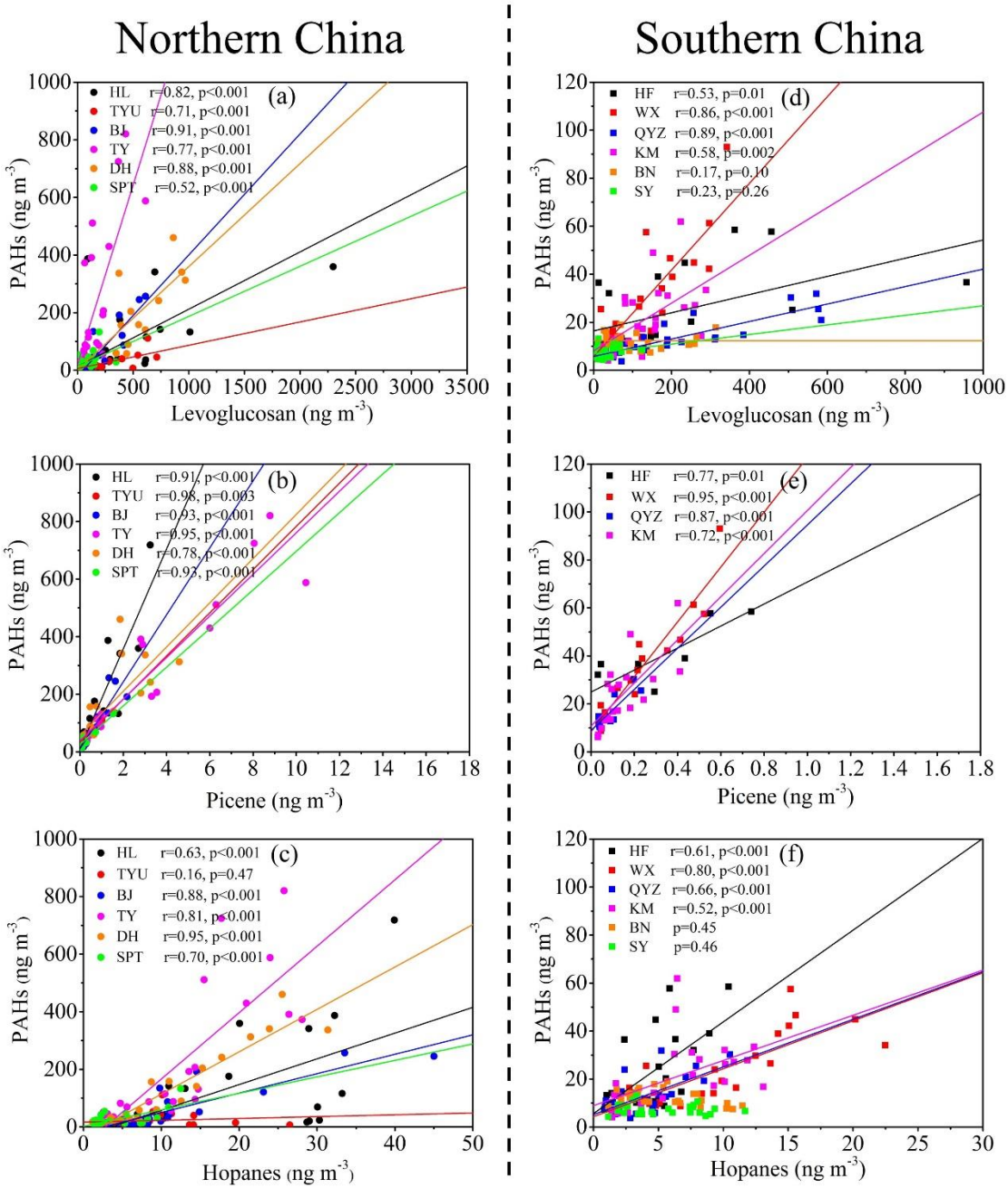

768

769 Figure 6 The correlation between PAHs and levoglucosan, picene and hopanes at sites in the

770 northern China (a-c) and the southern China (d-f).

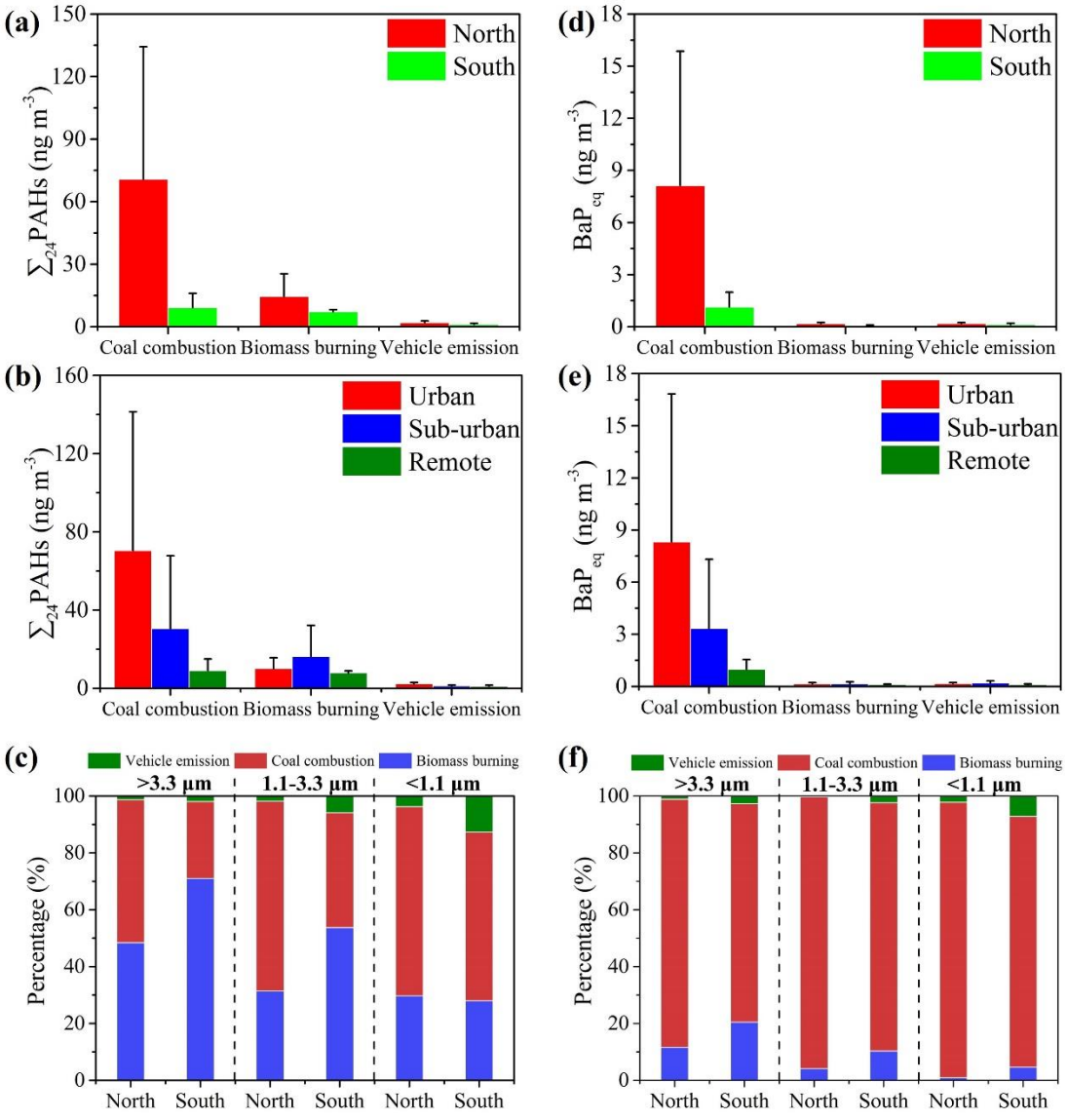

771

772 Figure 7 Source apportionment of $\sum_{24}$ PAHs and BaP_{eq} in different regions (a, c), sampling sites

773 (b, d) and size particles (c, f).

774

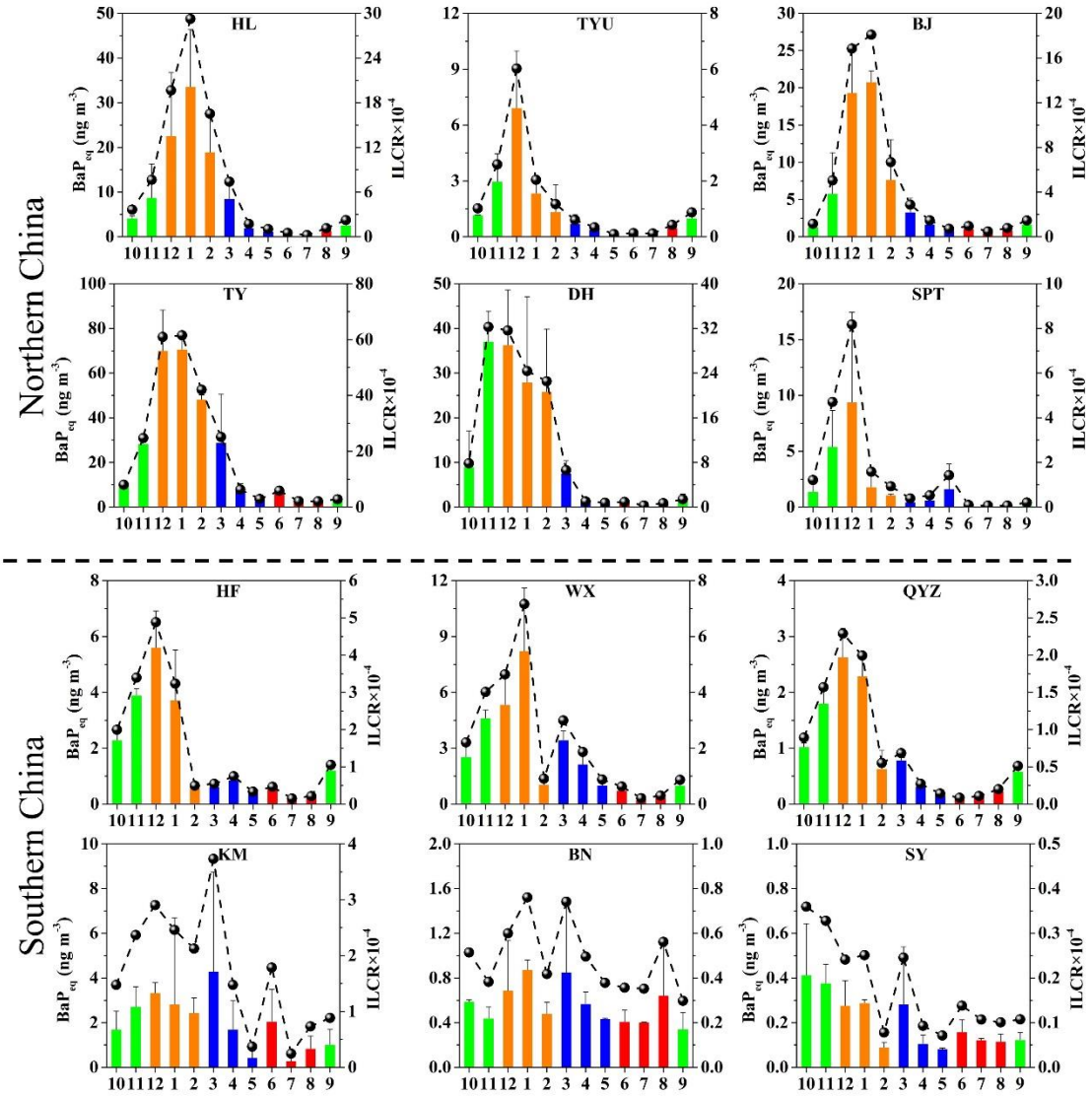

Figure 8 Monthly variations of BaP_{eq} and ILCR at sites in the northern China and the southern China. The green, yellow, blue and red bars represent BaP_{eq} in fall (October − November, 2012 and September, 2013), winter (December 2012 – February 2013), spring (March – May, 2013), and summer (June − August, 2013), respectively.

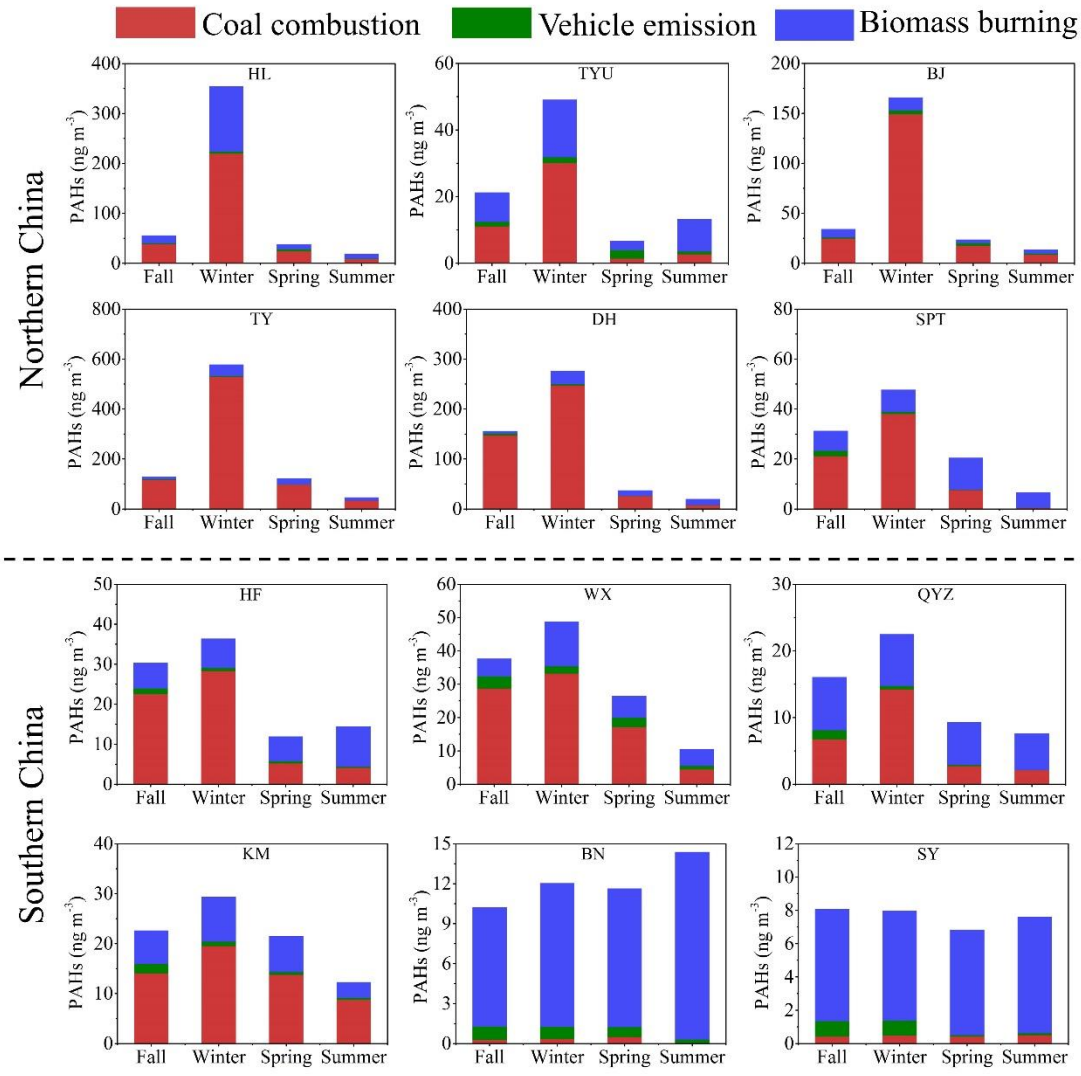

Figure 9 Seasonal variations of PAHs source contributions in China.